Hirshikesh *et al. Asia Pac. J. Comput. Engin. (2017) 4:3*
DOI 10.1186/s40540-017-0020-3

Asia Pacific Journal on Computational Engineering

RESEARCH Open Access

Trefftz polygonal finite element for linear elasticity: convergence, accuracy, and properties

Hirshikesh[1], S. Natarajan[1*], R. K. Annabattula[1], S. Bordas[2] and E. Atroshchenko[3]

*Correspondence:
snatarajan@iitm.ac.in
[1] Department of Mechanical Engineering, Indian Institute of Technology-Madras, Chennai, India
Full list of author information is available at the end of the article

Abstract

In this paper, the accuracy and the convergence properties of Trefftz finite element method over arbitrary polygons are studied. Within this approach, the unknown displacement field within the polygon is represented by the homogeneous solution to the governing differential equations, also called as the T-complete set. While on the boundary of the polygon, a conforming displacement field is independently defined to enforce the continuity of the field variables across the element boundary. An optimal number of T-complete functions are chosen based on the number of nodes of the polygon and the degrees of freedom per node. The stiffness matrix is computed by the hybrid formulation with auxiliary displacement frame. Results from the numerical studies presented for a few benchmark problems in the context of linear elasticity show that the proposed method yields highly accurate results with optimal convergence rates.

Keywords: Trefftz finite element, Polytopes, T-complete functions, Boundary integration

Background

Wachspress [1] introduced the concept of defining basis functions on any wedge form, which also yields interpolants on polytopes of any convex shapes. These shape functions are unconventional when compared to the polynomials used in the conventional finite elements. The use of elements with arbitrary number of sides provides flexibility in automatic mesh manipulation. For example, the domain can be discretized without a need to maintain a particular element topology. This is advantageous in adaptive mesh refinement, where a straightforward subdivision of individual elements usually results in hanging nodes. Traditionally, this is eliminated by introducing additional edges/faces to retain conformity. This can be alleviated if the computations are directly on meshes with hanging nodes. However, until recently elements with arbitrary number of sides did not find their applications in the computational mechanics, partly because of the associated difficulties with mesh generation and numerical integration. With the pioneering work of Alwood and Cornes [2], Sukumar and Tabarraei [3], Dasgupta [4], to name a few, now discretization of the domain with finite elements having arbitrary number of sides has gained increased attention [3, 5–10]. This has led to a new area of finite elements called '*polygonal finite elements*.' There are different techniques to compute the basis functions over arbitrary polygons. Some of them include (a) using length and area measures [1];

(b) natural neighbor interpolants [11]; (c) maximum entropy approximant [12]; and (d) harmonic shape functions [8]. As the approximation functions over arbitrary polygonal elements are usually non-polynomial (in particular, rational polynomials) which introduces difficulties in the numerical integration, improving numerical integration over polytopes has gained increasing attention [3, 13–15]. It is beyond the scope of this paper to review advances in polygonal finite element methods. Interested readers are referred to the literature [16, 17] and references therein for detailed discussion. Once the basis functions are constructed, the conventional Galerkin procedure is normally employed to solve the governing equations over the polygonal/polyhedral meshes.

Sukumar [18] used Voronoï cells and natural neighbor interpolants to develop a finite difference method on unstructured grids. Rashid and Gullet [19] proposed a variable element topology finite element method, in which shape functions for convex and non-convex elements are computed in the physical space using constrained minimization procedure. Based on the assumed stress hybrid formulation, Ghosh et al. [20] developed the Voronoï cell finite element method. Tiwary et al. [21] studied the behavior of microstructures with irregular geometries. Liu et al. [22–24] generalized the concept of strain smoothing technique to arbitrarily shaped polygons. The main idea is to write the strain as the divergence of a spatial average of the compatible strain field. On another front, a fundamental solution less method (Scaled Boundary Method) was introduced by Wolf and Song [25]. It shares the advantages of the FEM and the boundary element method (BEM). Like the FEM, no fundamental solution is required, and like the BEM, the spatial dimension is reduced by one, since only the boundary needs to be discretized, resulting in a decrease in the total degrees of freedom. Ooi et al. [26] employed scaled boundary formulation in polygonal elements to study crack propagation.

Apart from the aforementioned formulations, recent studies, among others, include developing polygonal elements based on the virtual nodes [27] and the virtual element methods [28]. The other possible approach is to employ basis functions that satisfy the differential equation locally [29, 30]. This method has been studied in detail in [31, 32] and extended to higher order polygons in [5, 33]. Zienkiewicz [34] presented a concise discussion on different approximation procedures to differential equations. It was shown that Trefftz-type approximation is a particular form of weighted residual approximation. This can be used to generate *hybrid finite elements*. Earlier studies employed boundary-type approximation associated with Trefftz to develop special type finite elements, for example, elements with holes/voids [35, 36], for plate analysis [37–39]. Recently, the idea of employing local solutions over arbitrary finite elements has been investigated in [5, 31–33]. However, its convergence properties and accuracy when applied to linear elasticity need to be investigated.

In this paper, hybrid Trefftz arbitrary polygons will be formulated and its convergence properties and accuracy will be numerically studied with a few benchmark problems in the context of linear elasticity. An optimal number of T-complete functions are chosen based on the number of nodes of the polygon and degrees of freedom per node. The salient features of the approach are (a) only the boundary of the element is discretized with 1D finite elements, and (b) explicit form of the shape functions and special numerical integration scheme are not required to compute the stiffness matrix.

The paper commences with an overview of the governing equations for elasticity and the corresponding Galerkin form. Section "Overview of hybrid Trefftz finite element

method" introduces a hybrid Trefftz-type approximation over arbitrary polytopes. The efficiency, the accuracy, and the convergence properties of the HTFEM (Hybrid Trefftz Finite Element Method) are demonstrated with a few benchmark problems in section "Numerical examples". The numerical results from the HTFEM are compared with the analytical results and with the polygonal FEM with Laplace/Wachspress interpolants, followed by concluding remarks in the last section.

Governing equations and weak form

For a 2D static linear elasticity problem defined in the domain Ω bounded by $\Gamma = \Gamma_u \bigcup \Gamma_t$, $\Gamma_u \bigcap \Gamma_t = \emptyset$, in the absence of body forces, the governing equation is given by

$$\nabla \cdot \boldsymbol{\sigma} = \mathbf{0} \quad \text{in} \quad \Omega \tag{1}$$

with the following conditions prescribed on the boundary:

$$\begin{aligned} \mathbf{u} &= \bar{\mathbf{u}} \quad \text{in} \quad \Gamma_u \\ \boldsymbol{\sigma} \cdot \mathbf{n} &= \bar{\mathbf{t}} \quad \text{on} \quad \Gamma_t \end{aligned}, \tag{2}$$

where $\boldsymbol{\sigma}$ is the stress tensor. The discrete equations for this problem are formulated from the Galerkin weak form:

$$\int_{\Omega} (\nabla \mathbf{u})^{\mathrm{T}} \mathbf{D} (\nabla \delta \mathbf{u}) \, \mathrm{d}\Omega - \int_{\Gamma_t} (\delta \mathbf{u})^{\mathrm{T}} \bar{\mathbf{t}} \, \mathrm{d}\Gamma = \mathbf{0}, \tag{3}$$

where $\mathbf{u}$ and $\delta\mathbf{u}$ are the trial and the test functions, respectively, and $\mathbf{D}$ is the material constitutive matrix. The FEM uses the following trial and test functions:

$$\mathbf{u}^h(\mathbf{x}) = \sum_{I=1}^{NP} \mathbf{N}_I(\mathbf{x}) \mathbf{d}_I, \quad \delta\mathbf{u}^h(\mathbf{x}) = \sum_{I=1}^{NP} \mathbf{N}_I(\mathbf{x}) \delta\mathbf{d}_I, \tag{4}$$

where NP is the total number of nodes in the mesh, $\mathbf{N}$ is the shape function matrix, and $\mathbf{d}_I$ is the vector of degrees of freedom associated with node I. Upon substituting Eq. (4) into Eq. (3) and invoking the arbitrariness of $\delta\mathbf{u}$, we obtain the following discretized algebraic system of equations:

$$\mathbf{K}\mathbf{d} = \mathbf{f} \tag{5}$$

with

$$\begin{aligned} \mathbf{K} &= \int_{\Omega^h} \mathbf{B}^{\mathrm{T}} \mathbf{D} \mathbf{B} \, \mathrm{d}\Omega \\ \mathbf{f} &= \int_{\Gamma_t} \mathbf{N}^{\mathrm{T}} \bar{\mathbf{t}} \, \mathrm{d}\Gamma, \end{aligned} \tag{6}$$

where $\mathbf{K}$ is the stiffness matrix and Ω^h is the discretized domain formed by the union of elements Ω^e. The stiffness matrix is computed over each element and assembled to the global matrix. The size of the stiffness matrix depends on the number of nodes in an element.

Generalization to arbitrary polygons

The growing interest in the generalization of FE over arbitrary meshes has opened up a new area of finite elements called '*polygonal finite elements*.' In polygonal finite elements, the number of sides of an element is not restricted to three or four as in the case of 2D. The Voronoï tessellation is a fundamental geometrical construct to generate a polygonal mesh covering a given domain. Polygonal meshes can be generated from Voronoï diagrams. The Voronoï diagram is a subdivision of the domain into regions $V(p_I)$, such that any point in $V(p_I)$ is closer to node p_I than to any other node. Figure 1 shows a Voronoï diagram of a point P. The first-order Voronoï $V(N)$ is a subdivision of the Euclidean space $\mathbb{R}^2$ into convex regions, mathematically:

$$T_I = \left\{ \mathbf{x} \in \mathbb{R}^2 : d(\mathbf{x}, \mathbf{x}_I) < d(\mathbf{x}, \mathbf{x}_J) \forall J \neq I \right\}, \tag{7}$$

where $d(\mathbf{x}_I, \mathbf{x}_J)$, the Euclidean matrix, is the distance between $\mathbf{x}_I$ and $\mathbf{x}_J$. The quality of the generated polygonal mesh depends on the randomness in the scattered points. Figure 2 shows a typical Voronoï tessellation of two sets of scattered dataset. The quality of a polygonal mesh determines the accuracy of the solution [3]. To improve the quality of the Voronoï tessellation, the generating point of each Voronoï cell can be used as its center of mass, leading to a special type of Voronoï diagram, called the centroidal Vornoï tessellation (CVT) [40]. Sieger et al. [41] presented an optimizing technique to improve the Voronoï diagrams for use in FE computations.

Overview of hybrid Trefftz finite element method

The basic idea in the Trefftz FEM is to employ the series of the homogeneous solution to the governing differential equation (see Eq. 1) as the approximation function to model the displacement field within the domain and an independent set of functions to represent the boundary and to satisfy inter-element compatibility (see Fig. 3). The set of

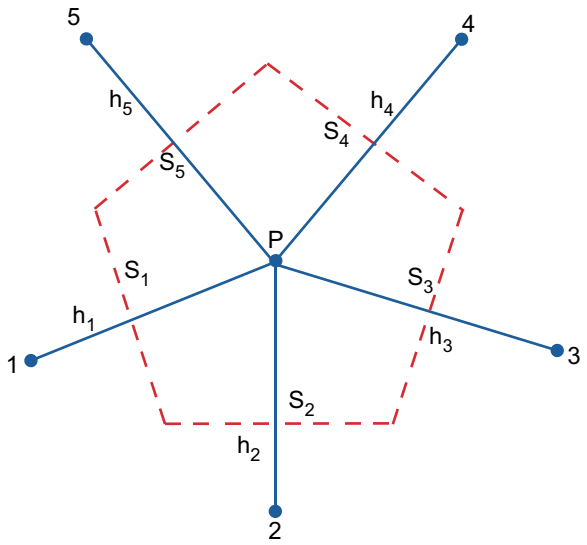

Fig. 1 Voronoï diagram of a point P

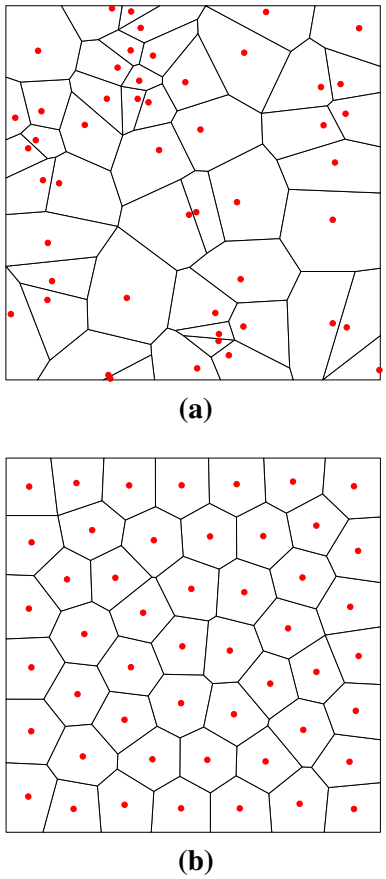

Fig. 2 Voronoï tessellation, where the *red dots* are the seed points: **a** scattered dataset; **b** polygonal mesh after few iterations

functions that are used to represent the displacement field within the domain are also called as T-complete set. The displacement field within an element can be written as

$$\mathbf{u} = \mathbf{N}\mathbf{c}, \quad \mathbf{x} \in \Omega, \tag{8}$$

where $\mathbf{c}$ are the vectors of undetermined coefficients and $\mathbf{N}_I$ are the approximation functions that are selected from the series solution of the homogeneous part of the governing differential equation (see Eq. 1). For linear elastostatics, based on the Mushelishvili's complex variable formulation, the $\mathbf{N}_I$ and the corresponding stress fields are given by [29]

$$\begin{aligned} \mathbf{N}_{Jk} &= \frac{1}{2G}\begin{Bmatrix} \mathrm{Re}Z_{Jk} \\ \mathrm{Im}Z_{Jk} \end{Bmatrix} \\ \mathbf{T}_{Jk} &= \begin{Bmatrix} \mathrm{Re}(R_{Jk} - S_{Jk}) \\ \mathrm{Re}(R_{Jk} + S_{Jk}) \\ \mathrm{Im}S_{Jk} \end{Bmatrix}, \end{aligned} \tag{9}$$

where $J = 1, 2, 3, 4, k = 1, 2, \ldots; Z_{1k} = i\kappa z^k + i\kappa z\bar{z}^{k-1}$, $Z_{2k} = \kappa z^k - kz\bar{z}^{k-1}$, $Z_{3k} = i\bar{z}^k$, and $Z_{4k} = -\bar{z}^k$; $R_{1k} = 2ikz^{k-1}, R_{2k} = 2kz^{k-1}, R_{3k} = 0, R_{4k} = 0$; and $S_{1k} = ik(k-1)z^{k-2}\bar{z}, S_{2k} = k(k-1)z^{k-2}\bar{z}, S_{3k} = iKz^{k-1}, S_{4k} = kz^{k-1}$.

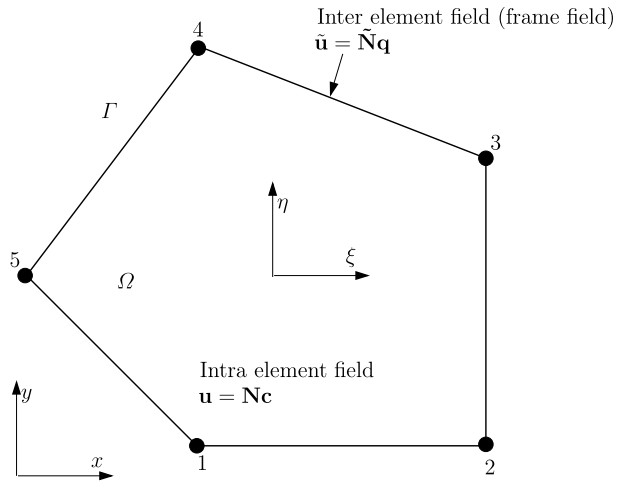

Fig. 3 Hybrid Trefftz polygonal element with a description of inter- and intra-element field

However, the intra-element displacement field given by Eq. (8) is non-conforming across the inter-element boundary. The unknown coefficients $\mathbf{c}$ are computed from the external boundary conditions and/or from the continuity conditions on the inter-element boundary. Of the various methods available to enforce these conditions, in this study, we use the hybrid technique. In this technique, the elements are linked through an auxiliary conforming displacement frame which has the same form as in the conventional FEM. The displacement field on the element boundary, or otherwise called frame, is given by

$$\tilde{\mathbf{u}} = \tilde{\mathbf{N}}\mathbf{q}, \quad \mathbf{x} \in \Gamma, \tag{10}$$

where $\mathbf{q}_I$ are the unknowns of the problem and $\tilde{\mathbf{N}}_I$ are the standard 1D FE shape functions. To satisfy the inter-element continuity, a modified variational form is employed [29], given by:

$$\Pi = \frac{1}{2}\int_{\Omega} \boldsymbol{\sigma}^{\mathrm{T}}\mathbf{D}^{-1}\boldsymbol{\sigma}\ \mathrm{d}\Omega - \int_{\Gamma_{e1}} \mathbf{t}\delta\mathbf{u}\ \mathrm{d}\Gamma + \int_{\Gamma_{e2}} (\bar{\mathbf{t}} - \mathbf{t})\mathbf{u}\ \mathrm{d}\Gamma - \int_{\Gamma_{eI}} \mathbf{t}\delta\tilde{\mathbf{u}}\ \mathrm{d}\Gamma, \tag{11}$$

where Γ_{eI} is the inter-element boundary, $\Gamma_{e1} = \Gamma_u \cap \Gamma_e$, and $\Gamma_{e2} = \Gamma_\sigma \cap \Gamma_e$. The minimization of the modified variational principle given by Eq. (11) leads to the following system of algebraic equations:

$$\mathbf{K}\mathbf{d} = \mathbf{f}, \tag{12}$$

where

$$\mathbf{K} = \mathbf{G}^{\mathrm{T}}\mathbf{H}^{-1}\mathbf{G}$$
$$\mathbf{F} = \int_{\Gamma} \tilde{\mathbf{N}}\bar{\mathbf{t}}\ \mathrm{d}\Gamma,$$

and

$$\mathbf{H} = \int_{\Gamma} \mathbf{Q}^{\mathrm{T}}\mathbf{N}\,\mathrm{d}\Gamma; \quad \mathbf{G} = \int_{\Gamma} \mathbf{Q}^{\mathrm{T}}\tilde{\mathbf{N}}\,\mathrm{d}\Gamma,$$

where $\mathbf{Q} = \mathbf{AT}$, and

$$\mathbf{A} = \begin{bmatrix} n_1 & 0 & n_2 \\ 0 & n_2 & n_1 \end{bmatrix} \quad \text{and} \quad \mathbf{T} = \nabla\mathbf{N},$$

where n_1 and n_2 are the outward normals. The integrals in the above equation can be computed by employing standard Gaussian quadrature rules. It is noted that in the computation of the stiffness matrix, we have to compute the inverse of the matrix $\mathbf{H}$. The necessary condition for the matrix $\mathbf{H}$ to be of full rank is

$$m_{\mathrm{mim}} = N_{\mathrm{dof}} - 1, \tag{13}$$

where N_{dof} is the total number of degrees of freedom of the element and m_{min} is the minimum number of T-complete functions to be used. Additionally, if m_{min} does not guarantee a matrix with full rank, full rank can be achieved by suitably increasing the number of T-complete functions.

Numerical examples

In this section, we present the convergence and accuracy of the arbitrary polygons with local Trefftz functions using benchmark problems in the context of linear elasticity. The results from the proposed approach are compared with analytical solution where available and with the conventional polygonal finite element method with Laplace interpolants. To discuss the results, we employ the following convention:

- *PFEM* Polygonal finite element method with Laplace/Wachspress interpolants (conventional approach). The numerical integration within each element is done by subdividing the polygon into triangles and employing a sixth-order Dunavant quadrature rule.
- *HT-PFEM* Hybrid Trefftz polygonal finite element method. Within each polygon, T-complete functions are employed to compute the stiffness matrix. One-dimensional Gaussian quadrature is employed along the boundary of the polygon and the order of the quadrature depends on the number of T-complete functions employed.

The built-in Matlab® function voronoin and Matlab® functions in PolyTop [42] for building the mesh-connectivity are used to create the polygonal meshes. Interested readers are referred to the corresponding author to obtain a MATLAB code for all the test cases presented in this manuscript. For the purpose of error estimation, we employ the relative error in the displacement norm and in the energy norm, given by:

Displacement norm

$$||\mathbf{u} - \mathbf{u}^h||_{L^2(\Omega)} = \frac{\sqrt{\int_{\Omega}(\mathbf{u} - \mathbf{u}^h)\cdot(\mathbf{u} - \mathbf{u}^h)\,\mathrm{d}\Omega}}{\sqrt{\int_{\Omega}\mathbf{u}\cdot\mathbf{u}\,\mathrm{d}\Omega}}. \tag{14}$$

Energy norm

$$||\mathbf{u}-\mathbf{u}^h||_{H^1(\Omega)} = \frac{\sqrt{\int_\Omega (\boldsymbol{\varepsilon}-\boldsymbol{\varepsilon}^h)^{\mathrm{T}}\mathbf{D}(\boldsymbol{\varepsilon}-\boldsymbol{\varepsilon}^h)\,\mathrm{d}\Omega}}{\sqrt{\int_\Omega \boldsymbol{\varepsilon}^{\mathrm{T}}\mathbf{D}\boldsymbol{\varepsilon}\,\mathrm{d}\Omega}}, \tag{15}$$

where $\mathbf{u}, \boldsymbol{\varepsilon}$ are the analytical solution or a reference solution and $\mathbf{u}^h, \boldsymbol{\varepsilon}^h$ are the numerical solution.

Cantilever beam bending

A two-dimensional cantilever beam was subjected to a parabolic shear load at the free end. The domain is discretized with arbitrary polygonal elements. See Fig. 4 for geometry, boundary conditions, and representative polygonal mesh. The geometry of the cantilever: length $L = 10$ and height $D = 2$. The material properties are as follows: Young's modulus, $E = 3\mathrm{e}^7$, Poisson's ratio $\nu = 0.25$, and the parabolic shear force $P = 150$. The exact solution for displacements is given by

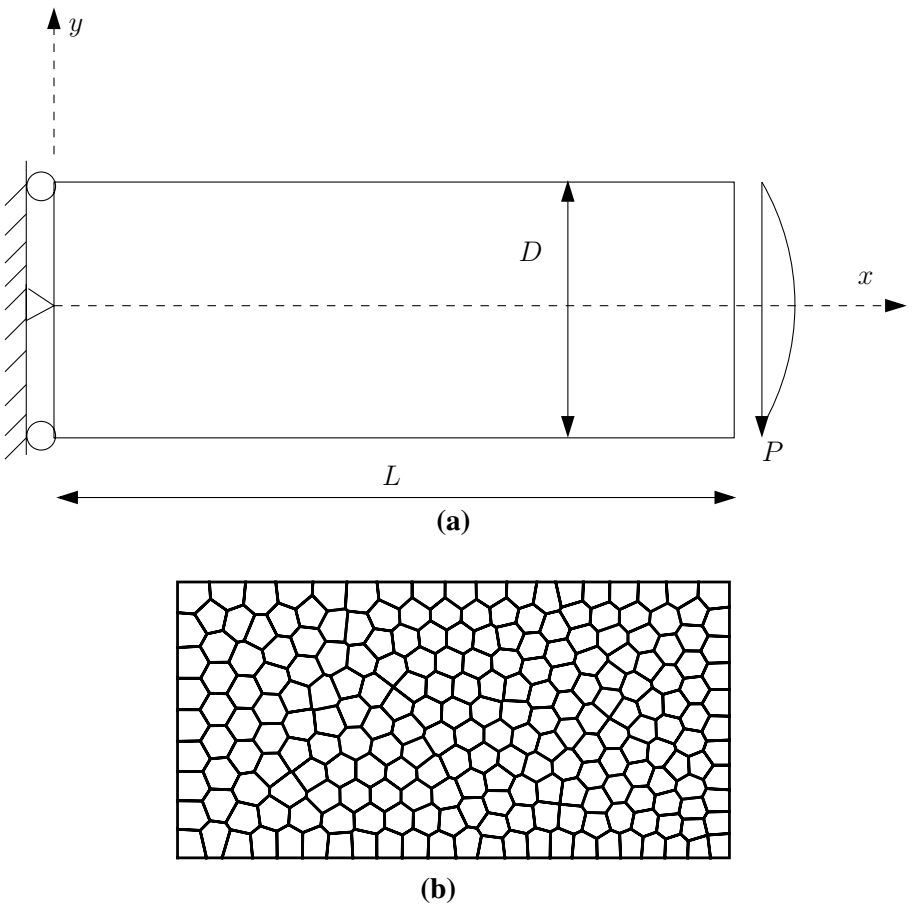

Fig. 4 Cantilever beam: **a** geometry and boundary conditions and **b** representative polygonal mesh. The domain is discretized with 100 elements

$$u(x,y) = \frac{Py}{6\overline{E}I}\left[(9L-3x)x + (2+\overline{\nu})\left(y^2 - \frac{D^2}{4}\right)\right]$$
$$v(x,y) = -\frac{P}{6\overline{E}I}\left[3\overline{\nu}y^2(L-x) + (4+5\overline{\nu})\frac{D^2x}{4} + (3L-x)x^2\right], \tag{16}$$

where $I = D^3/12$ is the moment of inertia, $\overline{E} = E$, $\overline{\nu} = \nu$, and $\overline{E} = E/(1-\nu^2)$, $\overline{\nu} = \nu/(1-\nu)$ for plane stress and plane strain, respectively.

The numerical convergence of the relative error in the displacement norm and the relative error in the energy norm are shown in Fig. 5. The results from the HT-PFEM and

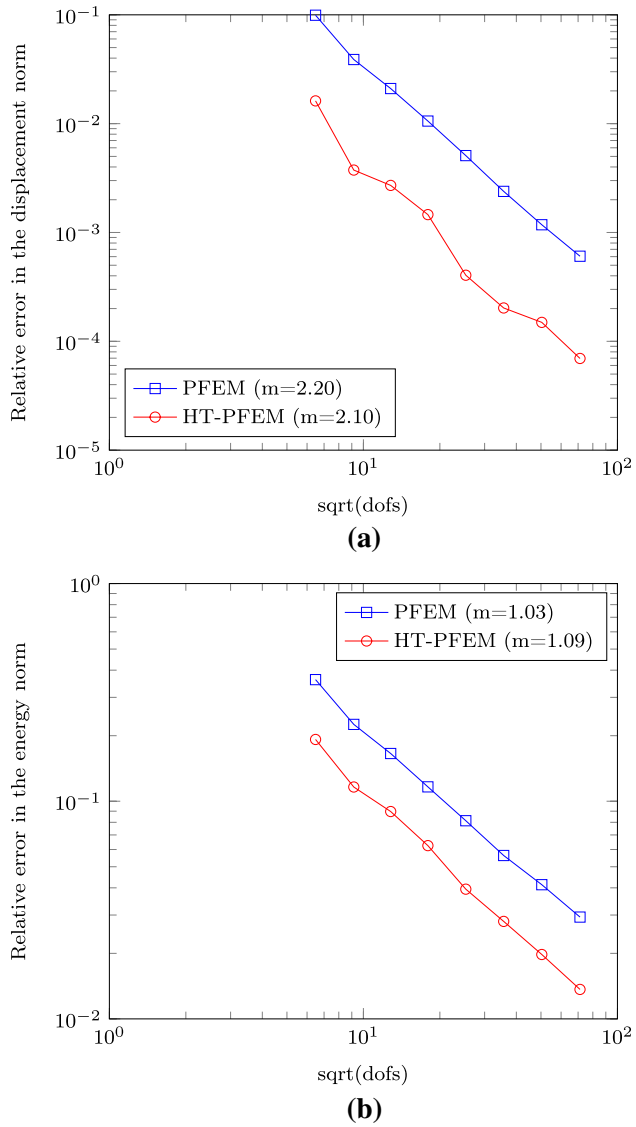

Fig. 5 Bending of thick cantilever beam: convergence results for **a** the relative error in the displacement norm (L^2) and **b** the relative error in the energy norm. The rate of convergence is also shown, where m is the average slope. In case of the polygonal SBFEM, p denotes the order of the shape functions along each edge of the polygon

Polygonal FEM are compared with the available analytical solution. Both the Polygonal FEM and the HT-PFEM yield optimal convergence in L^2 and H^1 norm. It is seen that with mesh refinement, both the methods converge to the exact solution. An estimation of the convergence rate is also shown. From Fig. 5, it can be observed that the HT-PFEM yields more accurate results and better convergence rate.

Infinite plate with a circular hole

In this example, consider an infinite plate with a traction free hole under uni-axial tension ($\sigma = 1$) along x-axis. See Fig. 6 for geometry description, boundary description, and representative polygonal mesh. The exact solution of the principal stresses in polar coordinates (r, θ) is given by

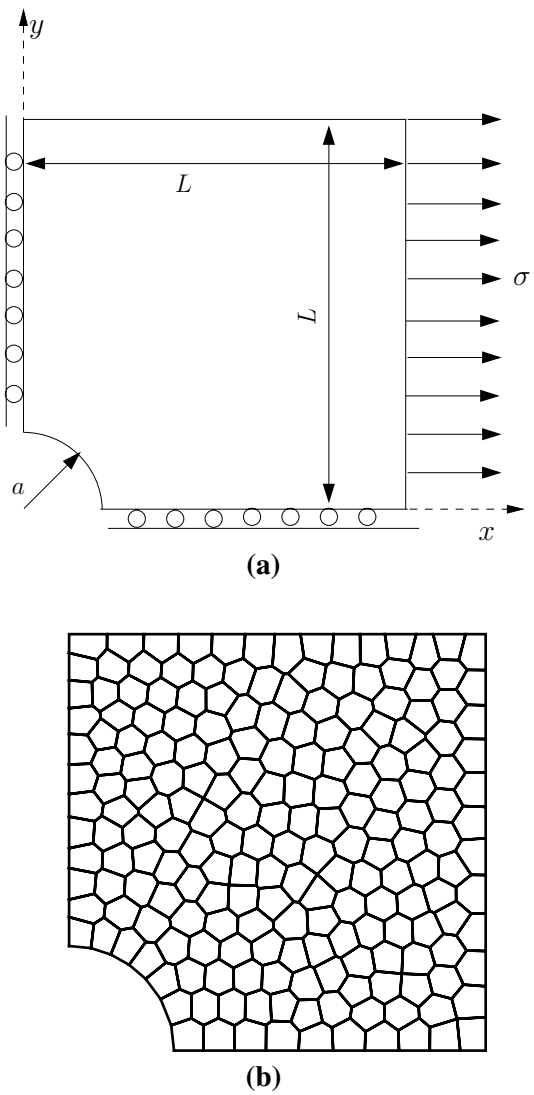

Fig. 6 Infinite plate with a circular hole: **a** geometry and boundary conditions and **b** representative polygonal mesh

$$\begin{aligned}
\sigma_{11}(r,\theta) &= 1 - \frac{a^2}{r^2}\left(\frac{3}{2}(\cos 2\theta + \cos 4\theta)\right) + \frac{3a^4}{2r^4}\cos 4\theta \\
\sigma_{22}(r,\theta) &= -\frac{a^2}{r^2}\left(\frac{1}{2}(\cos 2\theta - \cos 4\theta)\right) - \frac{3a^4}{2r^4}\cos 4\theta \\
\sigma_{12}(r,\theta) &= -\frac{a^2}{r^2}\left(\frac{1}{2}(\sin 2\theta + \sin 4\theta)\right) + \frac{3a^4}{2r^4}\sin 4\theta,
\end{aligned} \tag{17}$$

where a is the radius of the hole. Owing to symmetry, only one quarter of the plate is modeled. The material properties are as follows: Young's modulus $E = 10^5$ and Poisson's ratio $\nu = 0.3$. In this example, analytical tractions are applied on the boundary. The domain is discretized with polygonal elements, and along each edge of the polygon, the shape function is linear. The convergence rate in terms of the displacement norm is shown in Fig. 7. The relative error in the displacement norm for the PFEM and HT-PFEM is shown in Fig. 7. It can be seen that the HT-PFEM yields more accurate results when compared with the PFEM. The HT-PFEM yields slightly a better convergence rate when compared to the PFEM.

Circular beam

As a last example, consider a circular cantilevered beam subjected to a prescribed displacement $u_o = -0.01$ at the free end. The material property, boundary conditions considered for this study, and a representative polygonal mesh are shown in Fig. 8. The material is assumed to linear elastic and in a state of plane stress. The exact solution for the elastic energy is given by

$$U = \frac{1}{\pi}(\ln 2 - 0.6). \tag{18}$$

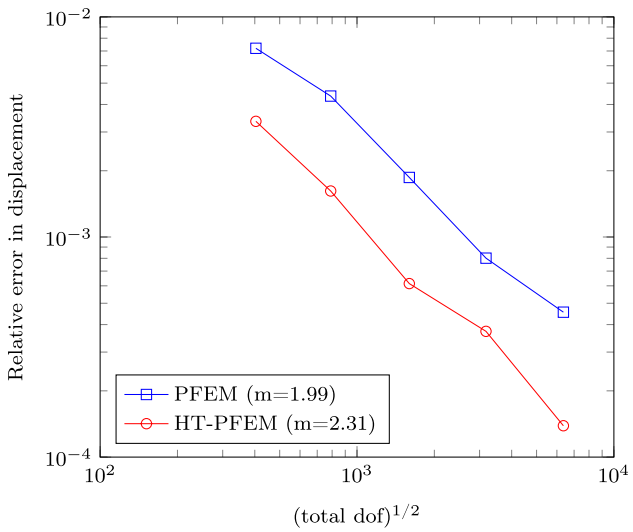

Fig. 7 Infinite plate with a circular hole: convergence results for the relative error in the displacement norm (L^2). The rate of convergence is also shown, where m is the average slope

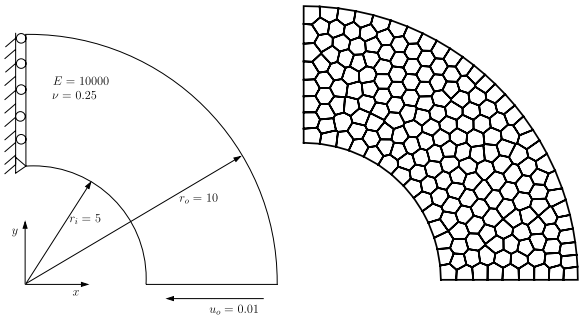

Fig. 8 Geometry, boundary conditions, and representative polygonal mesh for a curved cantilever circular beam. The displacements at the left end are constrained and a constant displacement is applied at the other end

The convergence in the relative error in the energy norm is shown in Fig. 9. It can be seen that the HT-PFEM yields more accurate results when compared with the PFEM. The HT-PFEM yields a convergence rate of 1.82 and the PFEM yields a convergence rate of 1.0. Both the methods converge to the exact energy with mesh refinement.

Next, we consider two problems with complex boundary: (a) a wrench and (b) a two-dimensional crane hook, both subjected to a concentrated force, $P = 210$ KN. The geometry, loading, and boundary conditions are shown in Figs. 10 and 11 for the wrench and the crane hook, respectively. The material properties are as follows: Young's modulus $E = 3e^7$ and Poisson's ratio $\nu = 0.3$. The domain is discretized with arbitrary polygonal elements. The appropriate number of T-functions and integration points are chosen based on the number of sides of the polygonal element. As these two problems do not

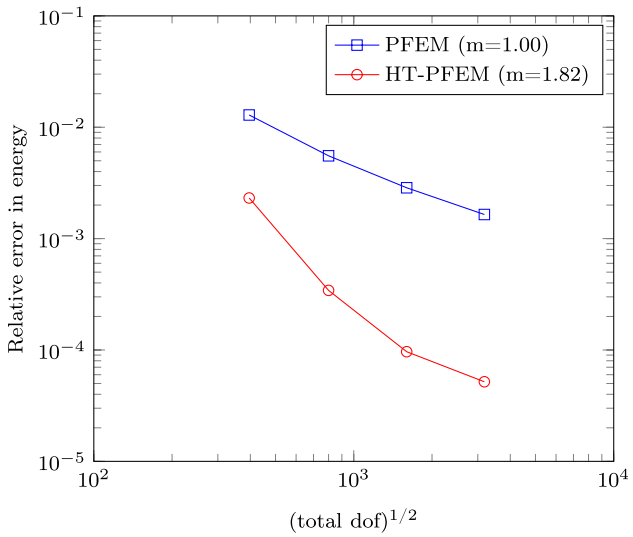

Fig. 9 Circular beam: convergence results for the relative error in the energy norm (L^2). The rate of convergence is also shown, where m is the average slope

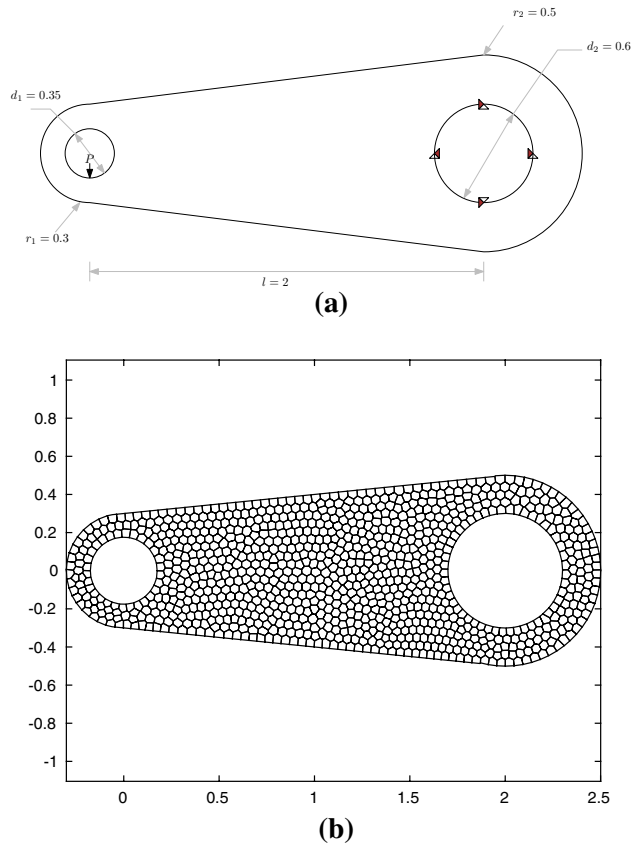

Fig. 10 A wrench subjected to point load: **a** geometry and boundary conditions and **b** representation polygonal mesh

have a closed form solution, we use the results from a FE simulation having 29,016 and 33,104 nodes for wrench and crane hook domain, respectively, as a reference solution. The convergence of the total strain energy with mesh refinement is shown in Fig. 12 for the wrench and crane hook domain. The results from the present method are compared with the results from the conventional PFEM. It is inferred that the present method converges faster than the conventional PFEM. Moreover, for the same number of degrees of freedom, the present method is more accurate than the PFEM with triangulation.

Concluding remarks

In this paper, we studied the convergence and accuracy of hybrid Trefftz polygonal finite elements. The hybrid Trefftz finite elements were constructed by employing the T-complete set of functions and a set of independent auxiliary field on the boundary. From the numerical studies presented, it is seen that hybrid Trefftz finite elements yield

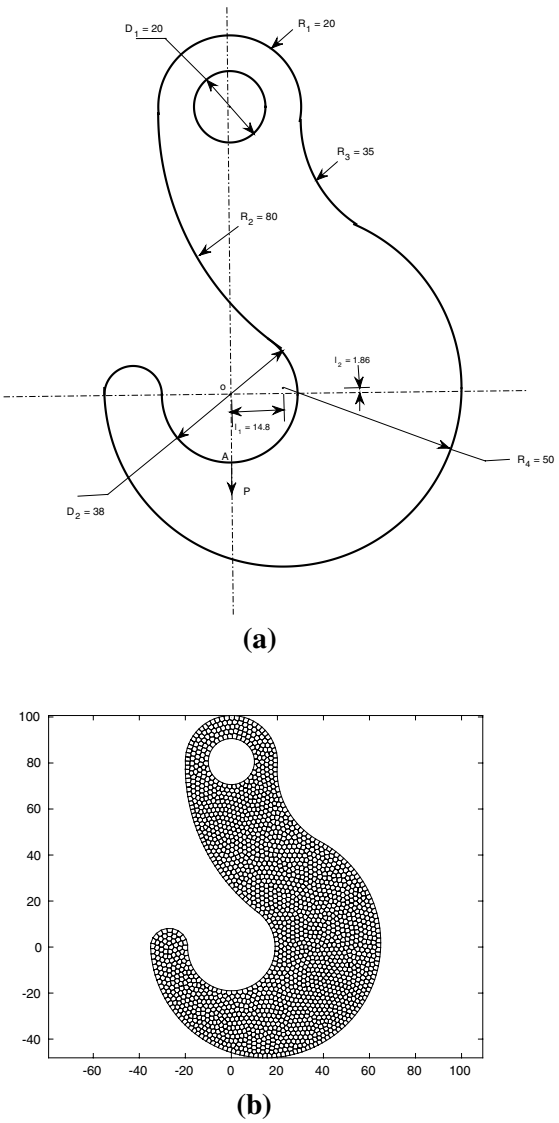

Fig. 11 A crane hook subjected to concentrated force: **a** geometry and boundary conditions and **b** representative mesh

more accurate results and better convergence rate when compared to the conventional polygonal finite elements with Laplace interpolants. One of the salient features of the hybrid Trefftz approach is that special finite elements with embedded cracks/voids can be constructed. This can then be combined with the extended finite element method to

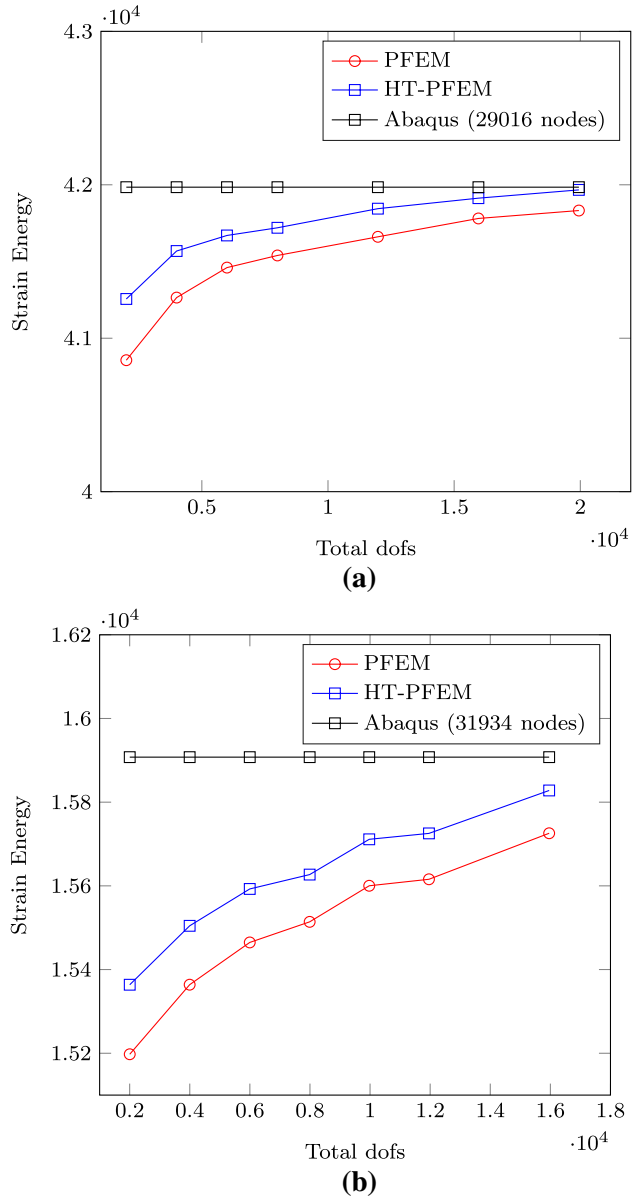

Fig. 12 Convergence of the total strain energy with mesh refinement: **a** wrench domain and **b** crane hook

model strong and weak discontinuities and singularities within the domain. However, the success of the method relies on the knowledge of T-complete function. This is a topic for future communication.

Authors' contributions

H is a Ph.D. student jointly supervised by SN and RKA, Department of Mechanical Engineering, IIT-Madras. SB and EA are external collaborators who helped in clarifying various aspects of the implementation of the method. All authors read and approved the final manuscript.

Author details

[1] Department of Mechanical Engineering, Indian Institute of Technology-Madras, Chennai, India. [2] Faculte des Sciences, de la Technologie et de la Communication, University of Luxembourg, Luxembourg, Luxembourg. [3] Department of Mechanical Engineering, University of Chile, Santiago, Chile.

Acknowledgements
No funding was received for this project.

Competing interests
The authors declare that they have no competing interests.

Publisher's Note

Springer Nature remains neutral with regard to jurisdictional claims in published maps and institutional affiliations.

Received: 10 August 2016 Accepted: 3 May 2017
Published online: 25 May 2017

References

1. Wachspress E (1971) A rational basis for function approximation. Springer, New York
2. Alwood R, Cornes G (1969) A polygonal finite element for plate bending problems using the assumed stress approach. Int J Numer Methods Eng 1:135
3. Sukumar N, Tabarraei A (2004) Conforming polygonal finite elements. Int J Numer Methods Eng 61:2045
4. Dasgupta G (2003) Interpolants within convex polygons: Wachspress' shape functions. J Aerosp Eng (ASCE) 16(1):1
5. Rjasanow S, Weißer S (2012) Higher order BEM-based FEM on polygonal meshes. SIAM J Numer Anal 50:2357
6. Barros FB, de Barcellos CS, Duarte CA (2007) p-Adaptive C k generalized finite element method for arbitrary polygonal clouds. Comput Mech 41:175
7. da Veiga LB, Brezzi F, Cangiani A, Manzini G, Marini L, Russo A (2013) Basic principles of virtual element methods. Maths Models Methods Appl Sci 23:199
8. Bishop J (2013) A displacement-based finite element formulation for general polyhedra using harmonic shape functions. Int J Numer Methods Eng 97:1. doi:10.1002/nme.4562
9. Biabanaki S, Khoei A (2012) A polygonal finite element method for modeling arbitrary interfaces in large deformation problems. Comput Mech 50:19. doi:10.1007/s00466-011-0668-4
10. Biabanaki S, Khoei A, Wriggers P (2013) Polygonal finite element methods for contact-impact problems on non-conformal meshes. Comput Methods Appl Mech Eng 269:198. doi:10.1016/j.cma.2013.10.025
11. Sukumar N, Moran B, Belytschko T (1998) The natural element method in solid mechanics. Int J Numer Methods Eng 43(5):839
12. Sukumar N (2013) Quadratic maximum-entropy serendipity shape functions for arbitrary planar polygons. Comput Methods Appl Mech Eng 263:27
13. Natarajan S, Bordas S, Mahapatra DR (2009) Numerical integration over arbitrary polygonal domains based on Schwarz-Christoffel conformal mapping. Int J Numer Methods Eng 80:103
14. Mousavi S, Xiao H, Sukumar N (2010) Generalized Gaussian quadrature rules on arbitrary polygons. Int J Numer Methods Eng 82(1):99
15. Talischi C, Paulino GH (2013) http://arxiv.org/pdf/1307.4423v1.pdf. **(In review)**
16. Fries T, Matthies H (2003) Classification and overview of meshfree methods. Tech. Rep. D38106, Institute of Scientific Computing, Technical University, Braunschweig, Hans-Sommer-Strasse
17. Sukumar N, Malsch E (2006) Recent advances in the construction of polygonal finite element interpolants. Arch Comput Methods Eng 13(1):129
18. Sukumar N (2003) Voronoi cell finite difference method for the diffusion operator on arbitrary unstructured grids. Int J Numer Methods Eng 57:1
19. Rashid M, Gullet P (2000) On a finite element method with variable element topology. Comput Methods Appl Mech Eng 190(11–12):1509
20. Moorthy S, Ghosh S (2000) Adaptivity and convergence in the Voronoi cell finite element model for analyzing heterogeneous materials. Comput Methods Appl Mech Eng 185:37
21. Tiwary A, Hu C, Ghosh S (2007) Numerical conformal mapping method based Voronoi cell finite element model for analyzing microstructures with irregular heterogeneities. Finite Elem Anal Design 43:504
22. Liu G, Nguyen T, Dai K, Lam K (2007) Theoretical aspects of the smoothed finite element method (SFEM). Int J Numer Methods Eng 71(8):902
23. Dai K, Liu G, Nguyen T (2007) An n-sided polygonal smoothed finite element method (nSFEM) for solid mechanics. Finite Elem Anal Design 43:847
24. Nguyen-Thoi T, Liu G, Nguyen-Xuan H (2011) An n-sided polygonal edge-based smoothed finite element method (nES-FEM) for solid mechanics. Int J Numer Methods Eng 27:1446
25. Wolf J, Song C (2001) The scaled boundary finite-element method—a fundamental solution-less boundary—element method. Comput Methods Appl Mech Eng 190:5551
26. Ooi ET, Song C, Tin-Loi F, Yang Z (2012) Polygon scaled boundary finite elements for crack propagation modelling. Int J Numer Methods Eng 91:319
27. Tang X, Wu S, Zheng C, Zhang J (2009) A novel virtual node method for polygonal elements. Appl Math Mech 30(10):1233
28. da Veiga L, Brezzi F, Cangiani A, Manzini G, Marini L, Russo A (2013) Basic principles of virtual element methods. Math Models Methods Appl Sci 23:199
29. Qin Q (2005) Trefftz finite element method and its applications. Appl Mech Rev 58:316
30. Copeland D, Langer U, Pusch D (2009) In: Bercovier M, Gander M, Komhuber R, Widlund O (eds). Lecture notes in Computational Science and Engineering, vol. 70

31. Hofreither C, Langer U, Pechstein C (2010) Analysis of a non-standard finite element method based on boundary integral operators. Elect Trans Num Anal 37:413
32. Weißer S (2011) Residual error estimate for BEM-based FEM on polygonal meshes. Numerische Math 118:765
33. Weißer S (2012) Finite element methods with local trefftz trial functions. Ph.D. thesis, Universität des Saarlandes, Saarbrücken
34. Zienkiewicz OC (1997) Trefftz type approximation and the generalized finite element method—history and development. Comput Assis Mech Eng Sci 4:305
35. Piltner R (1985) Special finite elements with holes and internal cracks. Int J Numer Methods Eng 21:1471
36. Qin QH, He XQ (2009) Special elliptic hole elements of Trefftz FEM in stress concentration analysis. J Mech MEMS 1:335
37. Jirousek J, Wróblewski A, Qin Q, He X (1995) A family of quadrilateral hybrid-Trefftz p-elements for thick plate analysis. Comput Methods Appl Mech Eng 127:315
38. Qin Q (1995) Hybrid-Trefftz finite element method for Reissner plates on an elastic foundation. Comput Methods Appl Mech Eng 122:379
39. Choo YS, Choi N, Lee BC (2010) A new hybrid-Trefftz triangular and quadrilateral plate elements. Appl Math Model 34:14
40. Du Q, Wang D (2005) Anisotropic centroidal Voronoi tessellations and their applications. SIAM J Sci Comput 26(3):737
41. Sieger D, Alliez P, Botsch M (2010) In: Proceedings of the 19th International Meshing Roundtable, pp. 335–350
42. Talischi C, Paulino GH, Pereira A, Menezes IF (2012) PolyTop: a Matlab implementation of a general topology optimization framework using unstructured polygonal finite element meshes. Struct Multidiscip Optim 45:329